Redox Biology 28 (2020) 101330

Contents lists available at ScienceDirect

Redox Biology

journal homepage: www.elsevier.com/locate/redox

Differential contribution of Nox1, Nox2 and Nox4 to kidney vascular oxidative stress and endothelial dysfunction in obesity

Mercedes Muñoz[a,1], Maria Elvira López-Oliva[a,1], Claudia Rodríguez[a], María Pilar Martínez[b], Javier Sáenz-Medina[c], Ana Sánchez[a], Belén Climent[a], Sara Benedito[a], Albino García-Sacristán[a], Luis Rivera[a], Medardo Hernández[a], Dolores Prieto[a,*]

[a] Departamento de Fisiología, Facultad de Farmacia, Universidad Complutense, Madrid, Spain
[b] Departamento de Anatomía y Embriología, Facultad de Veterinaria, Universidad Complutense, Madrid, Spain
[c] Departamento de Urología, Hospital Universitario Puerta de Hierro-Majadahonda, Madrid, Spain

ARTICLE INFO

Keywords:
Endothelial dysfunction
Renal arteries
Oxidative stress
Nox1
Nox4
Nox2
Obesity

ABSTRACT

Oxidative stress-associated endothelial dysfunction is a key pathogenic factor underlying the microvascular complications of metabolic disease. NADPH oxidase (Nox) is a major source of oxidative stress in diabetic nephropathy and chronic kidney disease, despite Nox4 and Nox2 have been identified as relevant sources of vasodilator endothelial H_2O_2.The present study was sought to investigate the role of Nox enzymes in renal vascular oxidative stress and endothelial dysfunction in a rat model of genetic obesity. Endothelial function was assessed in intrarenal arteries of obese Zucker rats (OZR) and their counterparts lean Zucker rats (LZR) mounted in microvascular myographs, and superoxide ($O_2^{\cdot-}$) and H_2O_2 production were measured. Impaired endothelium-dependent relaxations to acetylcholine (ACh) were associated to augmented $O_2^{\cdot-}$ generation, but neither ROS scavengers nor the Nox inhibitor apocynin significantly improved these relaxant responses in renal arteries of OZR. Whereas NO contribution to endothelial relaxations was blunted, catalase-sensitive non-NO non-prostanoid relaxations were enhanced in obese rats. Interestingly, NADPH–dependent $O_2^{\cdot-}$ production was augmented while NADPH-dependent H_2O_2 generation was reduced, and cytosolic and mitochondrial SOD were up-regulated in kidney of obese rats. Nox4 was down-regulated in renal arteries and Nox4-dependent H_2O_2 generation and endothelial relaxation were reduced in OZR. Up-regulation of both Nox2 and Nox1 was associated with augmented $O_2^{\cdot-}$ production but reduced H_2O_2 generation and blunted endothelial Nox2-derived H_2O_2-mediated in obese rats. Moreover, increased Nox1-derived $O_2^{\cdot-}$ contributed to renal endothelial dysfunction in OZR. In summary, the current data support a main role for Nox1-derived $O_2^{\cdot-}$ in kidney vascular oxidative stress and renal endothelial dysfunction in obesity, while reduced endothelial Nox4 expression associated to decreased H_2O_2 generation and H_2O_2–mediated vasodilatation might hinder Nox4 protective renal effects thus contributing to kidney injury. This suggests that effective therapies to counteract oxidative stress and prevent microvascular complications must identify the specific Nox subunits involved in metabolic disease.

1. Introduction

Oxidative stress is key pathogenic factor underlying the vascular complications of metabolic disease including diabetes- and obesity-related nephropathy and leading to the development and progression of kidney injury [1,2]. Both mitochondria and NADPH oxidases (Nox) are accepted as major sources of ROS generation in diabetic nephropathy and chronic kidney disease, but the specific role of the various Nox subunits in kidney injury remains controversial, since certain Nox enzymes have been implicated in both physiological and pathological renal processes. Thus, Nox2 participates in renal tubular functions such as electrolyte transport and glucose handling [3], while both Nox2 and Nox4 have recently been shown to be sources of endothelium-derived vasodilator H_2O_2 in renal arteries [4]. On the other hand, Nox4 or *renox,* the most abundantly expressed Nox isoform in the kidney, has consistently been found up-regulated and associated to kidney fibrosis in diabetes, therefore being proposed as the most critical Nox isoform linked to diabetic nephropathy [5–8]. In contrast, other studies have

* Corresponding author. Departamento de Fisiología, Facultad de Farmacia, Universidad Complutense de Madrid, 28040, Madrid, Spain.
E-mail address: dprieto@ucm.es (D. Prieto).
[1] MM and ELO equally contributed to this work.

https://doi.org/10.1016/j.redox.2019.101330
Received 10 July 2019; Received in revised form 27 August 2019; Accepted 16 September 2019
Available online 20 September 2019

Abbreviations

ACh	acetylcholine;
COX	cyclooxygenase
EC	endothelial cell
EDH	endothelium-derived-hyperpolarization
eNOS	endothelial nitric oxide synthase
H_2O_2	hydrogen peroxide
LZR	Lean Zucker rat
NADPH	nicotinamide adenine dinucleotide phosphate
NO	nitric oxide
NOS	nitric oxide synthase
Nox	NADPH oxidase enzymes
OZR	Obese Zucker rat
$O_2^{\cdot}$	superoxide
Phe	phenylephrine
PSS	physiological saline solution
ROS	reactive oxygen species
SOD	superoxide dismutase
VSM	vascular smooth muscle

demonstrated that renal expression of Nox4 is decreased in the course of diabetes and this isoform is crucial for kidney tubular cell survival under injury conditions [9–11]. Moreover, studies in Nox2-and Nox4-deficient animals do not appear to involve these Nox isoforms as major drivers of renal disease [9,12].

Obesity is a public health problem of increasing prevalence worldwide and a risk factor for the development of chronic kidney disease (CKD) independent of diabetes, hypertension and other comorbidities [13,14]. Microalbuminuria progressing to overt proteinuria is the earliest indication of obesity-related renal dysfunction, and glomerular hypertrophy and hyperfiltration develop in parallel to increasing body mass in obese individuals [15,16]. On the other hand, obesity is accepted as a state of low-grade systemic inflammation and oxidative stress is the trigger of renal inflammation that promotes the progression of obesity-associated kidney injury [17,18]. Mitochondria and Nox4 are the two major sources of ROS in the kidney [2,19]. Thus, mitochondria-derived oxidative stress has been associated to kidney proinflammatory and structural changes in response to lipid overload in high fat diet (HFD)-fed mice [20], while mitochondrial protection prevents renal inflammation, glomerulopathy and obesity associated-renal injury [21]. Increased ROS production in mesangial, endothelial and tubular cells mostly derived from Nox4 have been found associated to both diabetes- [7] and obesity-related kidney disease [22], linked to stimulation of TFG-β and matrix genes and to activation of profibrotic processes underlying fibrosis in diabetic nephropathy [6,7].

Oxidative stress in plasma and renal vascular tissue has also been involved in the reduced NO levels and impaired endothelial function of renal arterioles from genetic and HFD-induced models of obesity [18,23]. While COX-2, a mediator of renal inflammation, has been identified as a key source of ROS leading to enhanced vasoconstriction and endothelial dysfunction in renal arteries of obese rats [23], the specific contribution of Nox-derived ROS remains to be elucidated due to the controversy on the implication of Nox2 and Nox4 in both physiological and pathophysiological processes in the kidney. Therefore, the present study was sought to investigate the contribution of Nox enzymes to renal vascular oxidative stress and endothelial dysfunction in obesity. We used the obese Zucker rat (OZR), a well stablished model of genetic obesity/metabolic syndrome that exhibits glomerular hypertrophy and proteinuria by 12–14 weeks age and develops glomerulosclerosis with increasing age ultimately leading to renal failure [24,25].

2. Materials and methods

2.1. Animal model

In the present study, 8–10 weeks of age Male obese Zucker rats (OZR) (fa/fa) and their control counterparts, lean Zucker rats (LZR) (fa/-) were purchased from Charles River RMS (Spain). Rats were housed at the Pharmacy School animal care facility and maintained on standard chow and water ad libitum, until they were used for study, at 17–18 weeks of age. All animal care and experimental protocols conformed to the European Union Guidelines for the Care and the Use of Laboratory Animals (European Union Directive 2010/63/EU) and were approved by the Institutional Animal Care and Use Committee of Madrid Complutense University. Animals were killed and the kidneys quickly removed and placed in cold (4 °C) physiological saline solution (PSS) of the following composition (mM): NaCl 119, $NaHCO_3$ 25, KCl 4.7, KH_2PO_4 1.17, $MgSO_4$ 1.18, $CaCl_2$ 1.5, EDTA 0.027 and glucose 11, continuously gassed with a mixture of 5% CO_2/95% O_2 to maintain pH at 7.4. On the day of the experiment, blood samples were obtained and plasma was frozen for determination of non-fasting glucose, cholesterol, triglycerides and insulin plasma levels by using commercially available kits. Plasma insulin levels were measured by specific enzyme-linked immunosorbent assay.

2.2. Dissection and mounting of microvessels

Renal interlobar arteries, second- or third order branches of the renal artery from LZR and OZR, were carefully dissected by removing the medullary connective tissue and mounted in parallel in double microvascular myographs (Danish Myotechnology, Denmark) by inserting two 40 μm tungsten wires into the vessel lumen. After mounting the arteries were equilibrated for 30 min in PSS maintained at 37 °C. The relationship between passive wall tension and internal circumference was determined for each individual artery and from this, the internal circumference, L_{100} corresponding to a transmural pressure of 100 mmHg for a relaxed vessel *in situ* was calculated. The arteries were set to an internal diameter L_1 equal to 0.9 times L_{100} (L_1 = 0.9 x L_{100}), since force development in intrarenal arteries is close to maximal at this internal lumen diameter.

2.3. Experimental procedures for the functional experiments

At the beginning of each experiment, arteries were challenged twice with 120 mM K^+ solution (KPSS) in order to test vessel viability. Endothelium-dependent vasodilatation of renal arteries was assessed by the relaxant effects of acetylcholine (ACh) upon addition of cumulative concentrations of this agent on arteries precontracted with phenylephrine (Phe) in the absence and presence of the SOD scavenger tempol (30 μM), the specific mitochondrial superoxide scavenger

Table 1
Plasma metabolic and renal function parameters of LZR and OZR.

	LZR	n	OZR	n
Body weight (g)	388 ± 7	45	480 ± 7***	47
Weeks	17–18		17–18	
$[Glucose]_{blood}$ (mg/dl)	112 ± 10	8	139 ± 11*	11
$[Insulin]_{plasma}$ (ng/ml)	1.1 ± 0.1	6	3.93 ± 0.4***	6
$[Cholesterol]_{plasma}$ (mg/dl)	89 ± 4	8	184 ± 15***	10
$[Triglycerides]_{plasma}$ (mg/dl)	84 ± 9	8	310 ± 40***	10
$[Urea]_{plasma}$ (mg/dl)	35 ± 1	8	41 ± 1**	8
$[Creatinina]_{plasma}$ (mg/dl)	0.39 ± 0.04	8	0.40 ± 0.01	8

Data are means ± SEM of the number *n* of animals. Significant differences were analyzed by an unpaired Student *t*-test. *$P < 0.05$; **$p < 0.001$; ***$P < 0.0001$ *vs* LZR.

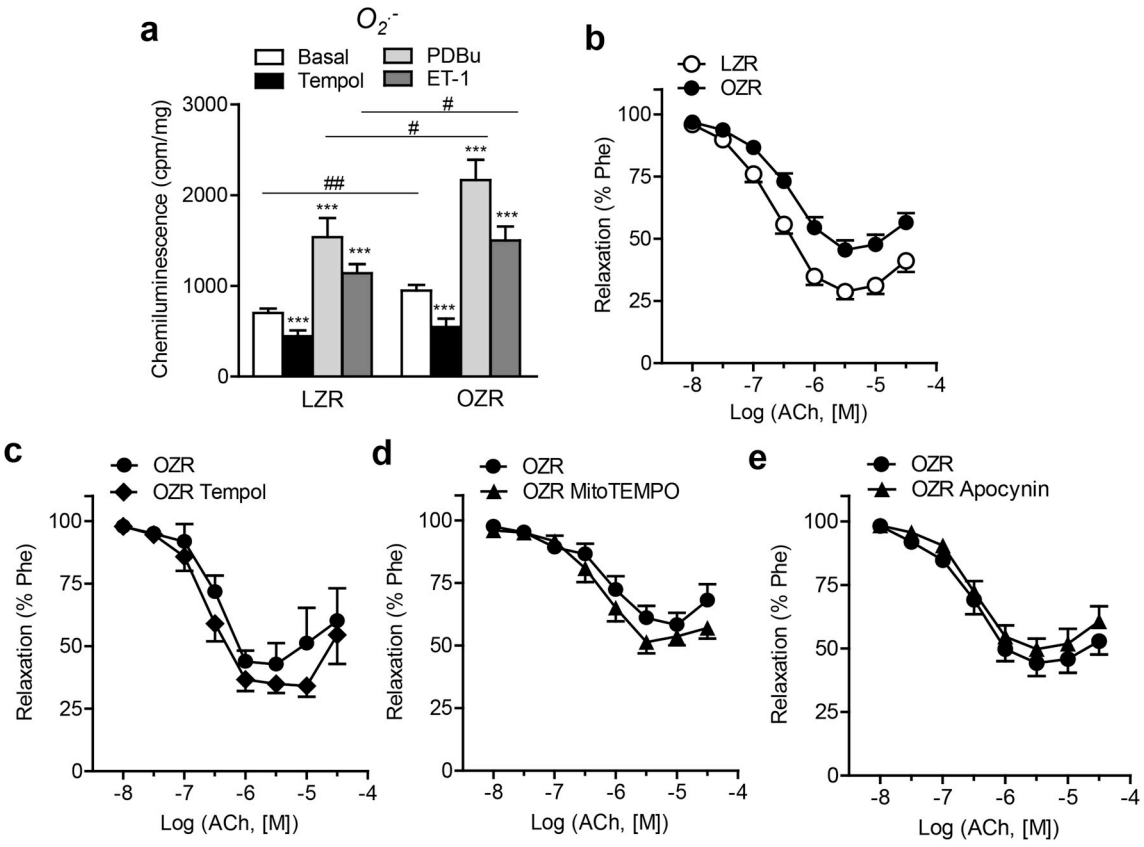

Fig. 1. Vascular oxidative stress and endothelial dysfunction resistant to ROS scavengers in renal arteries of obese rats. (a) Basal and PDBu and ET-1-stimulated $O_2^{\cdot-}$ production and effect the SOD mimetic tempol (100 μM) on basal superoxide production of rat renal interlobar arteries measured by lucigenin-enhanced chemiluminiscence. Results are expressed as counts per minute (cpm) per mg of tissue. Bars represent mean ± SEM of 7–20 animals. Statistically significant differences were calculated by unpaired Student *t-test* ***p < 0.001 *versus* basal levels. $^{\#}p < 0.05$; $^{\#\#}p < 0.01$ *versus* renal arteries of LZR. (b) Average relaxations to ACh in renal interlobar arteries from OZR compared to LZR. Effects of (c) the SOD mimetic tempol (30 μM), (d) the specific mitochondrial superoxide scavenger MitoTEMPO (1 μM) and (e) the Nox inhibitor apocynin (30 μM) on the relaxant responses to ACh of rat renal interlobar arteries from OZR. Results are expressed as percentage of the precontraction induced by phenylephrine (Phe). Data are shown as the mean ± SEM of 6–30 arteries. Significant differences were analyzed by paired Student *t-test* *p < 0.01 *versus* control before treatment.

MitoTEMPO (1 μM), the non-selective Nox inhibitor apocynin (30 μM), catalase (200 IU/mL) and L-NOARG (100 μM) and previously incubated with L-NOARG and indomethacin (1 μM) to block NOS and COX enzymes, respectively. The responses to exogenous ACh were further obtained and compared after treatment with the non-selective Nox 4 inhibitor plumbagin (1 μM), the dual Nox1/4 inhibitor GKT137831 (0.1 μM), the selective Nox2 inhibitor Nox2ds-tat (1 μM) and the selective Nox1 inhibitor NoxA1ds-tat (0.1 μM) [26]. The drugs were added to the myograph chamber 30 min before a second concentration-response curve was performed, and the Phe concentration was adjusted to match the contraction during the first control curve assessment.

2.4. Measurement of superoxide production by chemiluminescence

Changes in basal, ET-1-induced and NADPH-stimulated levels of $O_2^{\cdot-}$ were detected by lucigenin-enhanced chemiluminiscence, as previously described [4,23]. Cortex samples and 4–6 segments of the renal interlobar arteries about 4–5 mm long were dissected out from the kidney of LZR and OZR, equilibrated in PSS for 30 min at room temperature and then incubated in the absence (controls) and presence of the tempol (100 μM) to determine basal $O_2^{\cdot-}$ levels, and in the presence of the protein kinase C (PKC) activator phorbol 12,13-dibutyrate (PDBu) (30 μM) and of the vasoconstrictor peptide endothelin (ET-1) (0.01 μM) to measure ET-1-stimulated $O_2^{\cdot-}$ levels, that are greatly enhanced and contribute to vascular oxidative stress and endothelial dysfunction in obesity [27]. To assess Nox-stimulated $O_2^{\cdot-}$ generation, intact intrarenal arteries and cortex samples were incubated with extracellular NADPH (100 μM) for 30 min at 37 °C. Since CYP 2C epoxygenases also contribute to NADPH-dependent $O_2^{\cdot-}$ production in renal tissues [4], treatment with the selective Nox inhibitors Nox2ds-tat (1 μM), GKT137831 (0.3 μM) and NoxA1ds-tat (0.3 μM), was used to determine the relative contribution of the different Nox subunits to ROS generation in renal arteries and cortex from obese rats compared to controls. Samples were then transferred to microtiter plate wells containing 5 μM bis-N-methylacridinium nitrate (lucigenin) in the absence and presence of different ROS inhibitors and of stimulation with NADPH which was added previous to determination. Chemiluminescence was measured in a luminometer (BMG Fluostar Optima), and for calculation baseline values were subtracted from the counting values under the different experimental conditions and superoxide production was normalized to dry tissue weight.

2.5. Measurement of hydrogen peroxide by Amplex Red

Nox-derived H_2O_2 levels were measured by Amplex Red H_2O_2 assay Kit (Life Technologies) in renal arteries and cortex from LZR and OZR. Since apocycin is a non-selective Nox inhibitor that has additional peroxide scavenging properties besides its inhibitory action on Nox activity [28], selective Nox inhibitors were used in order to determine the relative contribution of Nox subunits to H_2O_2 production in renal tissues. Samples were equilibrated in HEPES-physiological saline solution (PSS) for 30 min at room temperature and then incubated with

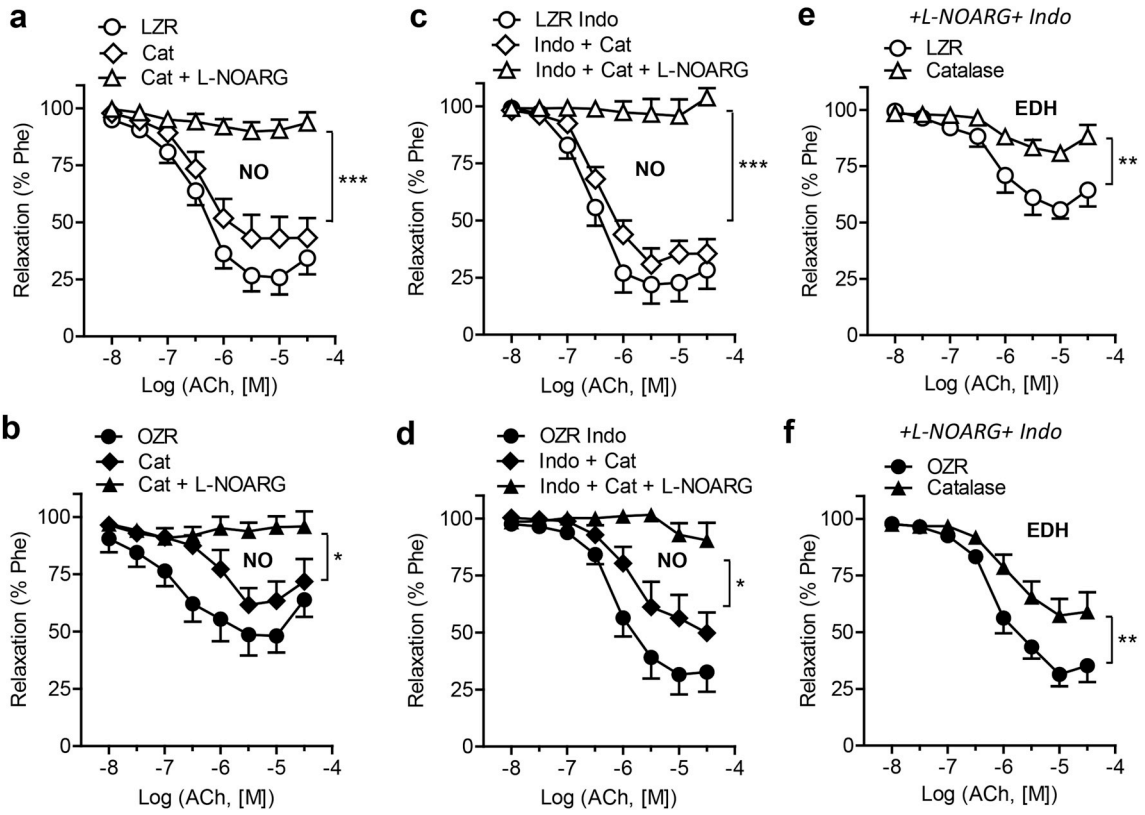

Fig. 2. Renal endothelial dysfunction involves impaired NO but enhanced non-NO no-prostanoid EDH type relaxations in obese rats. (a–d) Effects of catalase (cat, 200 U/ml) and catalase plus the NOS synthase inhibitor L-NOARG (100 μM) on the average relaxant responses to ACh in renal arteries from LZR (a,c) and OZR (b,d), in the absence (a,b) and presence (c,d) of COX inhibitor indomethacin (Indo, 0.3 μM). (e,f) Effect of catalase on the EDH-type relaxant responses elicited by the endothelial agonist acetylcholine (ACh) under conditions of NOS and COX blockade in renal arteries from LZR (e) and OZR (f). Results are expressed as percentage of the precontraction induced by phenylephrine (Phe). Data are shown as the mean ± SEM of 7–12 arteries. Significant differences were analyzed by paired Student *t-test* *p < 0.05 **p < 0.01 ***p < 0.001 *versus* catalase treated.

NADPH (100 μM) in the absence (controls) and presence of the Nox inhibitors Nox2ds-tat (1 μM), GKT137831 (0.3 μM), Nox1ds-tat (0.3 μM) and apocynin (30 μM) for 30 min at 37 °C. Arteries and cortex samples were then transferred to microtiter plate black wells containing 10 mM final concentration (Amplex Red) and 10 U/ml final concentration (horseradish peroxidase) in the absence and presence of different ROS sources inhibitors and some samples were stimulated with either NADPH just prior to determination. Fluorescence was measured in a fluorimeter (BMG Fluostar Optima), using an excitation filter of 544 nm and an emission filter of 590 nm. Background fluorescence was subtracted from the counting values under the different experimental conditions and H_2O_2 production was normalized to dry tissue weight.

2.6. Western blotting analysis of Nox subunits

Interlobar arteries and renal cortex samples from LZR and OZR were homogenized on ice in lyses buffer containing 10 mM Tris-HCl (pH 7.4), 1% SDS, 1 mM sodium vanadate and 0.01% protease inhibitor cocktail (Sigma Aldrich, Madrid, Spain). After centrifugation at 15000 × *g* for 20 min at 4 °C, proteins in the supernatants were quantified by the DC Protein Assay Kit (Bio-Rad, Madrid Spain). For each sample, 50 μg protein/lane was separated in a 10% polyacrylamide gel (SDS-PAGE) and transferred to a polyvinylidene fluoride (PVDF) membrane (GE Healthcare, Madrid, Spain). For immunodetection, membranes were incubated overnight at 4 °C with the polyclonal primary antibodies: anti-CuZnSOD, anti-MnSOD (1/1000), anti-catalase (1/1000) and anti-Nox4 (1/500) (Santa Cruz Biotechnology, Quimigen, Madrid, Spain), anti-Nox1 (1/500) and Nox2/gp91phox (1/1000) (Abcam, Cambridge, UK). The blots were also probed for β-actin (1/40000) as the loading control using a mouse monoclonal antibody (Sigma Aldrich, Madrid, Spain). After washed, bound primary antibody was detected with horseradish peroxidase conjugated secondary antibodies and blots were development by chemiluminescence (ECL Select-kit, GE Healthcare, Madrid, Spain) on ImageQuant LAS 500 imaging system (GE Healthcare, Madrid, Spain). Densitometry analysis was performed using Quantity One v4.62 software. Protein expression levels were normalized to β-actin.

2.7. Immunohistochemistry

Tissue samples from kidneys containing interlobar arteries and samples of renal cortex from LZR and OZR were immersion-fixed in 4% paraformaldehyde in 0.1 M sodium phosphate-buffer (PBS). Kidney paraffin embedded sections (4 μm) were deparaffinized and blocked for 10 min with 0.3% hydrogen peroxide at room temperature. After antigen retrieval and blocking, sections were incubated overnight at 4 °C with the following biotinylated primary antibodies: anti-CuZnSOD (1/200); anti-MnSOD (1/200); anti-catalase (1/200); anti-Nox1 (1/100); anti-Nox2/gp91phox (1/100) and anti-Nox4 (1/100). Immunochemical staining was performed using streptavidin-biotin conjugated horseradish peroxidase (HRP) (EMD Millipore Corp., Darmstadt, Germany) and visualised by incubation with 3, 3′-diaminobenzidine (DAB) (Sigma Aldrich, Madrid, Spain). The sections were counterstained by Harris's hematoxylin, dehydrated and mounted. Colocalization of Nox4 with eNOS in renal arteries wall was obtained in 5 μm thick transversal cryostat sections preincubated in 10% normal goat serum in PB containing 0.3% Triton-X-100 for 2–3 h. Nox4 expression was determined

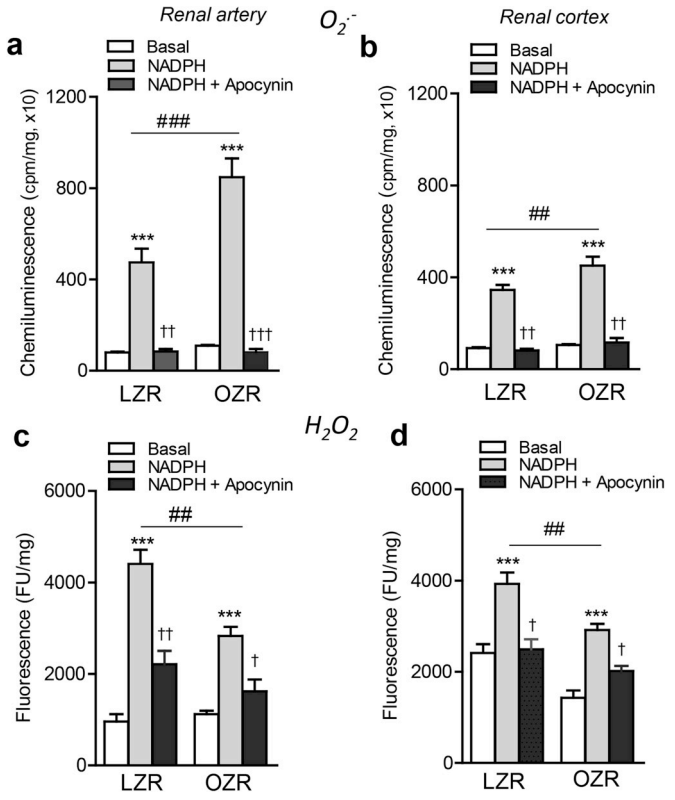

Fig. 3. Nox-dependent $O_2^{\cdot-}$ production is augmented while Nox-derived H_2O_2 generation is reduced in renal tissues of obese rats. (a–d) Basal and NADPH-stimulated $O_2^{\cdot-}$ and H_2O_2 production and effect of the non-selective Nox inhibitor apocynin (100 μM) in rat renal interlobar arteries and renal cortex from LZR and OZR, measured by lucigenin-enhanced chemiluminiscence (a,b) and Amplex Red fluorescence (c,d) assays, respectively. Results are expressed as counts per minute (cpm) per mg of tissue for chemiluminescence and relative fluorescence units (RFU) per mg of tissue. Bars represent mean ± SEM of 10–18 animals. Statistically significant differences were calculated by ANOVA followed by Bonferroni posterio test or unpaired Student's *t*-test ***p < 0.001 versus basal levels, †p < 0.05, ††p < 0.01 †††p < 0.001 versus NADPH-stimulated; #p < 0.05; ##p < 0.01; ###p < 0.001 versus LZR.

by immunofluorescence by incubating renal sections from LZR and OZR with a polyclonal primary antibody anti-Nox4 (1/100) (Santa Cruz Biotechnology, Quimigen, Madrid, Spain) and a mouse monoclonal anti-eNOS (Abcam, Cambridge, UK) diluted at 1:400 for 48 h, washed and allowed to react with a goat secondary serum (Chemicon International Inc) (anti-rabbit for the Nox4) diluted 1:200 for 3 h at room temperature. Secondary antibodies used were Alexa Fluor 594 (red) and Alexa Fluor 488 (green). The slides were covered with a specific medium containing DAPI, which stains all cell nuclei. The observations were made with a fluorescence microscope (Olympus IX51). No immunoreactivity could be detected in sections incubated in the absence of the primary antisera. Preadsorption with Nox proteins showed no cross-reactivity to the antibodies.

2.8. Data presentation and statistical analysis

For the functional experiments, results are expressed as either Nm^{-1} of tension or as a percent of the responses to either Phe or KPSS in each artery, as means ± SEM of 6–15 arteries (1–2 from each animal). For measurements of $O_2^{\cdot-}$ or H_2O_2 production, results are expressed as counts per minute (cpm) per mg of tissue and relative fluorescence units (RFU) per mg of tissue in arterial segments and cortex samples, respectively, as means ± SEM of 4–7 animals. The statistical differences between means were analyzed by using one-way ANOVA followed by Bonferroni's *post hoc* test for comparisons involving more than two groups or by paired or unpaired Student's *t*-test for comparison between two groups. Probability levels lower than 5% were considered significant. All calculations were made using a standard software package (Prism 6.0, GraphPad, San Diego, CA).

3. Results

3.1. General parameters

Metabolic profile and plasma renal function parameters are shown in Table 1. At the time of the experiment (17–18 weeks of age), OZR were significantly heavier than LZR and exhibited mild hyperglycemia, hyperinsulinemia and dyslipidemia with elevated total cholesterol and triglycerides levels. Renal function, as assessed by plasma creatinine and urea, remained normal (Table 1).

The normalized internal lumen diameters, l_1, of renal arteries in the OZR group (252 ± 9 μm, n = 30) were not significantly different from those in the LZR group (247 ± 14 μm, n = 23), thus supporting that structure is preserved in arteries from OZR compared to LZR. Vasoconstrictor response to KPSS (1.18 ± 0.18 Nm^{-1}, n = 23, in LZR and 1.18 ± 0.11, n = 30, in OZR) or Phe (1.31 ± 0.20 Nm^{-1}, n = 23, in LZR, and 1.28 ± 0.17, n = 30, in OZR) were also unchanged in OZR.

3.2. Oxidative stress and endothelial dysfunction resistant to antioxidants in renal arteries of OZR

Basal $O_2^{\cdot-}$ levels assessed by lucigenin chemiluminescence, and also those stimulated by ET-1 or PDBu, were significantly higher in renal arteries of OZR compared to LZR (Fig. 1a), thus showing vascular oxidative stress in the kidney of obese animals. Endothelial function was evaluated by the vasodilatador responses to acetylcholine (ACh) that were significantly impaired in renal interlobar arteries from obese rats (Fig. 1a). However, the endothelial relaxations elicited by ACh were not improved by acute treatment with either the SOD mimetic tempol (Fig. 1c), the mitochondrial ROS scavenger MitoTEMPO (Fig. 1d) or the non-selective Nox inhibitor apocynin (Fig. 1e) in OZR, despite augmented oxidative stress in renal arteries.

H_2O_2 has recently been involved along with NO in the endothelium-dependent relaxations of intrarenal arteries [4], and therefore the relative contribution of NO and H_2O_2 were determined in arteries from lean and obese animals in order to assess the nature of the impaired ACh relaxant responses. The NO-mediated component of the ACh relaxations, obtained in the presence of catalase (Fig. 2a and b) and enhanced by treatment with indomethacin to block COX-derived contractile prostanoids (Fig. 2c and d), was significantly reduced in arteries of OZR, thus confirming impaired vasodilator responses to NO in obese rats. Interestingly, a marked enhancement of the relaxations induced by ACh was unmasked when assessing endothelial relaxations under conditions of NOS and COX enzymes blockade (Fig. 2e and f), thus suggesting the involvement of compensatory non-NO non-prostanoid EDH type mechanisms in renal arteries from obese rats. However, H_2O_2 did not account for these enhanced relaxations since catalase nearly abolished the non-NO endothelial relaxant component in LZR but not in OZR (Fig. 2e and f).

3.3. Nox-derived $O_2^{\cdot-}$ production is elevated while Nox-derived H_2O_2 generation is decreased in renal arteries from obese rats

In order to assess the contribution of Nox-derived oxidative stress to renal endothelial dysfunction of obese rats, NADPH-stimulated $O_2^{\cdot-}$ and H_2O_2 production was measured by lucigenin chemiluminescence and Amplex Red fluorescence, respectively, in the absence and presence of the non-selective NOX inhibitor apocynin. Both $O_2^{\cdot-}$ and H_2O_2 levels were markedly enhanced by NADPH in both renal interlobar arteries

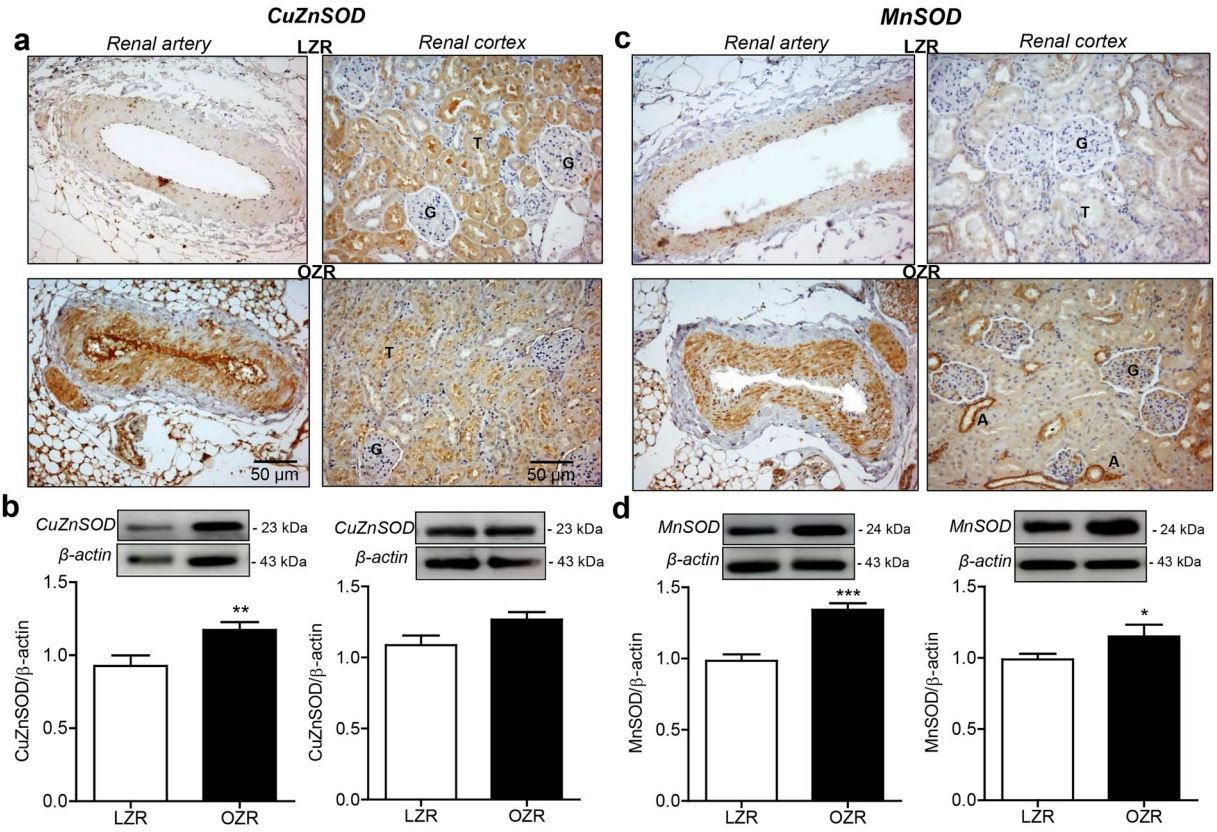

Fig. 4. Up-regulation of the H_2O_2-generating cytosolic and mitochondrial SOD in arterial and cortical renal tissues in obesity. (a,c) Inmunohistochemical demostration of CuZnSOD (a) and MnSOD (c) in renal interlobar artery and cortex from rat kidney of LZR and OZR. CuZnSOD and MnSOD were distributed throughout the endothelial lining and VSM of the renal interlobar artery, and in renal tubules (T) (CuZnSOD) and markedly up-regulated in arterioles (A) and glomeruli (G) (CuZnSOD) in the renal cortex of OZR compared to LZR. Sections are representative of n = 3 animals. (b,d) Western blot analysis of CuZnSOD and MnSOD expression in samples of renal artery and cortex showing that both proteins levels were higher in samples of renal cortex and renal arteries of OZR than in those of LZR. Results were quantified by densitometry and presented as a ratio of density of CuZnSOD and MnSOD bands vs those of β-actin from the sample. Data are shown as the mean ± SEM of 4 animals. Significant differences were analyzed using unpaired *t*-test *p < 0.05; **p < 0.01; ***p < 0.001 versus LZR.

and renal cortex (Fig. 3). Although a contribution of CYP epoxygenases to the enhanced NADPH-dependent ROS generation in obese rats cannot be ruled out [4], the marked inhibitory effect of apocynin on $O_2^{\cdot-}$ and to a lesser extent on H_2O_2 levels, suggests a major contribution of Nox to oxidative stress in renal tissues from OZR. Interestingly, while NADPH-stimulated $O_2^{\cdot-}$ levels abolished by apocynin were significantly larger in arteries, and to a lesser extent in renal cortex, of OZR compared to LZR (Fig. 3a and b), NADPH-stimulated H_2O_2 generation was significantly reduced in both arteries and cortex of obese rats compared to lean controls (Fig. 3c and d). Basal H_2O_2 levels were also significantly lower in renal cortex of obese rats. These data indicate that augmented Nox-derived $O_2^{\cdot-}$ generation contributes renal vascular oxidative stress, whereas kidney Nox-derived H_2O_2 production was decreased in obesity.

3.4. Up-regulation of vascular antioxidant defences in OZR

Vascular oxidative stress measured as increased $O_2^{\cdot-}$ generation in renal interlobar arteries was associated with the enhanced expression of the enzymes dismutating $O_2^{\cdot-}$ to H_2O_2, the cytosolic CuZnSOD (Fig. 4a and b) and the mitochondrial MnSOD (Fig. 4c and d) in the kidney of OZR, as depicted by the Western Blot analysis. Immunostaining of arterial sections further demonstrated that up-regulation of these antioxidant enzymes was particularly evident in VSM of obese rats (Fig. 4a,c). Western blot analysis and immunohistochemistry confirmed that catalase protein levels were also up-regulated and significantly higher in renal arteries from OZR compared to LZR but not in renal cortex (Supplementary Fig. 1).

3.5. Endothelial Nox4 expression, Nox4-derived H_2O_2 and Nox4-mediated endothelium-dependent relaxations are reduced in obese rats

In order to assess the relative contribution of the different Nox subunits to arterial oxidative stress and renal endothelial dysfunction in obese rats, Nox proteins were determined by Western blot and immunohistochemistry in renal interlobar arteries and cortex, and the effect of selective Nox inhibitors were evaluated on ROS production and on the H_2O_2-mediated endothelium-dependent relaxations of renal arteries [4].

Endothelial Nox4 has recently been identified as a physiological source of vasodilator H_2O_2 in renal arteries. Immunostaining of arterial sections showed that Nox4 was colocalized with eNOS protein in the endothelium of renal arteries from LZR (Fig. 5a and c), while Nox4 expression was reduced in the endothelium but it was found in VSM in OZR (Fig. 5a and c). No apparent differences in either distribution or density of the Nox4 immunolabeling were observed between LZR and OZR in renal cortex (Fig. 5b). Western blot analysis confirmed that total Nox4 protein levels were significantly reduced in renal arteries from obese rats compared to controls (Fig. 5d), while they were similar in cortical tissue of LZR and OZR (Fig. 5e).

The effect of the selective Nox1/4 inhibitor GKT137831 was next examined on ROS production of intrarenal arteries. GKT137831 reduced both $O_2^{\cdot-}$ (Fig. 6a) and H_2O_2 (Fig. 6b) formation stimulated by NADPH in LZR and OZR. This compound had a larger inhibitory effect on $O_2^{\cdot-}$ production in OZR (Fig. 6a), while the inhibitory effect on H_2O_2 generation was reduced in obese animals compared to controls (Fig. 6b). To determine whether changes in the Nox4 metabolism may

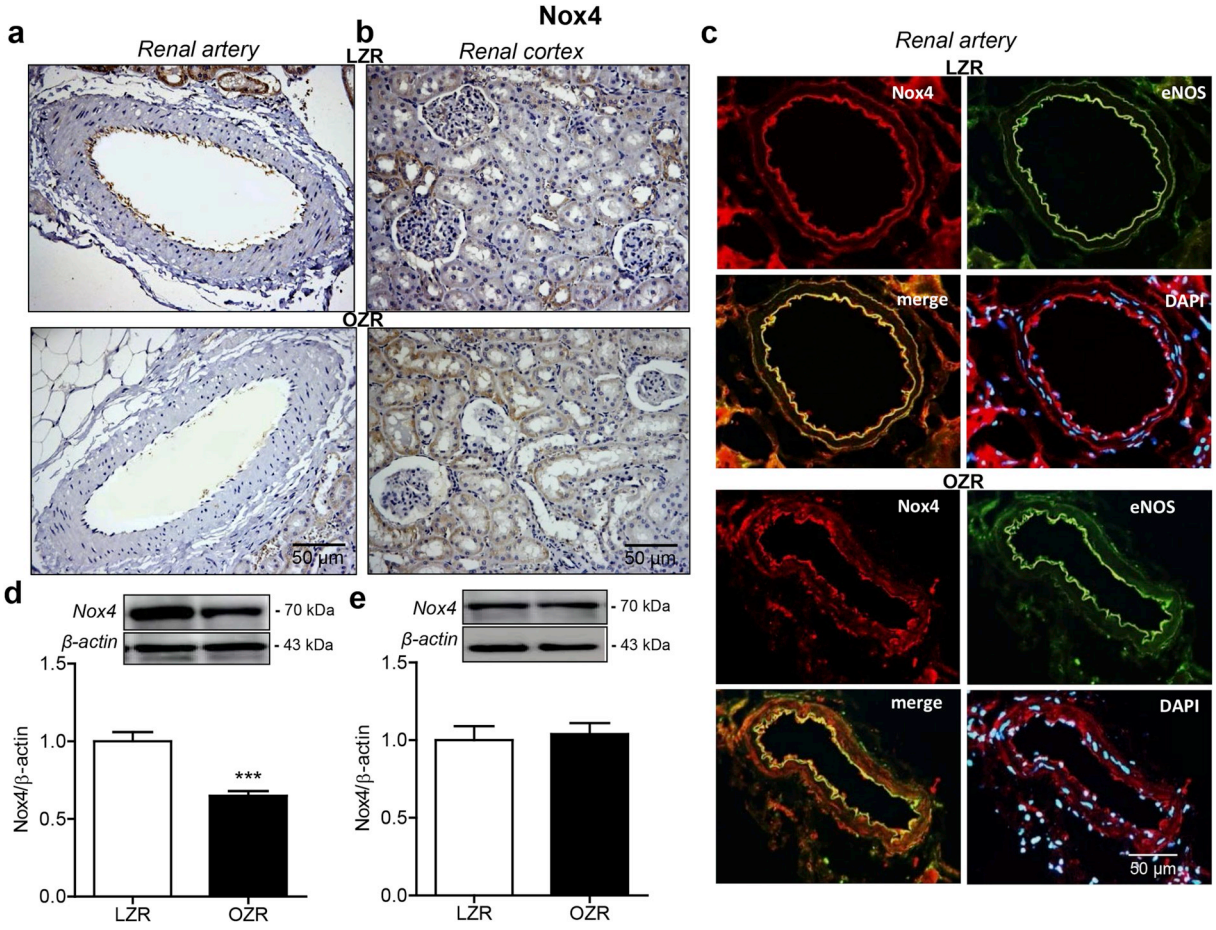

Fig. 5. Nox4 is down-regulated in renal arteries of obese rats. (a,b) Inmunohistochemical demostration of Nox4 in renal interlobar artery and cortex (glomeruli, tubules and arterioles) of the rat kidney from LZR and OZR. (c) Immunofluorescence double labelling for eNOS marker and Nox4 expression showing Nox4 protein (red areas) colocalized with eNOS (green areas) distributed throughout the endothelial lining of the renal interlobar artery in LZR, and to a lesser extent in the endothelium and extended to VSM in OZR. Scale bars indicate 50 μm. Sections are representative of n = 3 animals. (d,e) Western blot analysis of Nox4 expression in samples of renal artery and cortex showing that Nox4 protein levels were higher in samples of renal arteries from LZR than in those of OZR and there were no differences in samples of renal cortex from both animals. Results were quantified by densitometry and presented as a ratio of density of Nox4 band vs those of β-actin from the sample. Data are shown as the mean ± SEM of 4 animals. Significant differences were analyzed using unpaired *t*-test ***p < 0.001 versus LZR. (For interpretation of the references to colour in this figure legend, the reader is referred to the Web version of this article.)

be involved in the endothelial dysfunction observed in renal arteries of OZR, the effect of GKT137831 and of the non-selective Nox4 inhibitor plumbagin was assessed on the endothelium-dependent relaxations elicited by ACh. These relaxant responses were significantly inhibited by GKT137831 and by plumbagin in LZR (Fig. 6c and e) thus confirming the involvement of endothelial Nox4-derived H_2O_2 [4], but this inhibition was lesser in lean rats (Fig. 6d and f).

3.6. Up-regulation of arterial Nox2 is associated to reduced endothelial Nox2-derived H_2O_2 –mediated relaxations

Nox2-derived H_2O_2 is also involved in the endothelium-dependent relaxations of renal arteries [4] and its role in renal endothelial dysfunction of obese rats was assessed. Immunoreaction for Nox2 was found in interlobar arteries from LZR and OZR (Fig. 7a), while in renal cortex, Nox2 was widely distributed in tubular structures in LZR but its expression was markedly reduced in OZR (Fig. 7c). Western blot analysis showed higher Nox2 protein levels in rat intrarenal arteries of OZR compared to LZR (Fig. 7b), while there was a pronounced down-regulation of Nox2 in renal cortex of obese animals (Fig. 7d). The selective inhibitor of Nox2 Nox2ds-tat abolished $O_2^{\cdot-}$ production stimulated by NADPH in renal interlobar arteries of both LZR and OZR (Fig. 8a) and reduced H_2O_2 generation in LZR but hardly affect H_2O_2 production in OZR (Fig. 8b). To assess whether changes in Nox2-derived ROS may also contribute to renal endothelium dysfunction in OZR, renal arteries of LZR and OZR were treated with the selective Nox2 inhibitor Nox2ds-tat, which significantly reduced the relaxant responses in lean (Fig. 8c) but did not further affect these responses in renal arteries of obese rats (Fig. 8d).

3.7. Nox1 rather than Nox4 preferentially contributes to kidney vascular oxidative stress and endothelial dysfunction in obesity

Nox1 has recently been proposed to be the member of the NADPH oxidase family responsible for microvascular dysfunction in metabolic disease [29]. Nox1 protein was determined by immunohistochemistry and Western Blott in the kidney of LZR and OZR. Immunostaining of arterial samples with Nox1 antibodies revealed a very low expression of this subunit in renal arteries and cortex of LZR, but obesity markedly enhanced kidney Nox1 expression (Fig. 9a and c). Nox1 was found in VSM of renal arteries, and in both renal tubules and vascular tissue - glomeruli and arterioles- in samples of renal cortex of obese rats (Fig. 9a and c). Western Blott analysis confirmed that Nox1 protein levels were significantly up-regulated in isolated renal arteries (Fig. 9b) and renal cortex (Fig. 9d).of obese animals compared to controls.

Augmented NADPH-stimulated $O_2^{\cdot-}$ in renal arteries from OZR were

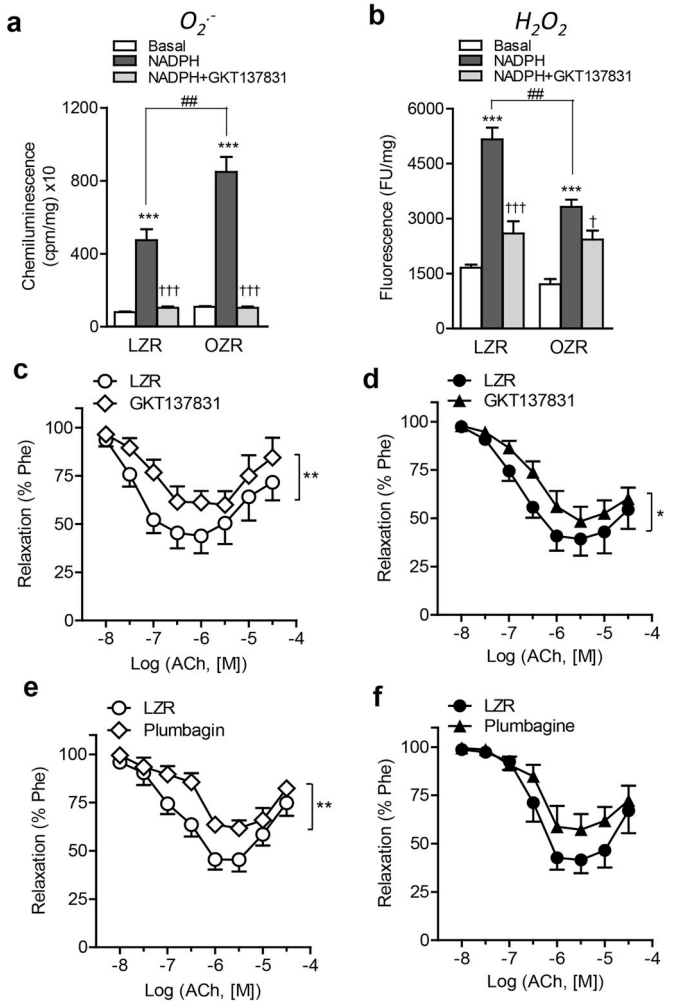

Fig. 6. The Nox4 inhibitors GKT137831 and plumbagin reduce ROS generation and endothelial H_2O_2-mediated relaxations in renal arteries of lean and to lesser extent of obese rats. (a,b) Effect of the Nox1/4 inhibitor GKT137831 (0.3 μM) on the NADPH-stimulated levels of $O_2^{\cdot-}$ (a) and H_2O_2 (b) measured by lucigenin-enhanced chemiluminescence and by Amplex Red fluorescence, respectively, in renal arteries of LZR and OZR. Results are expressed in counts per minute (cpm) per mg of tissue for chemiluminescence and in relative fluorescence units (RFU) per mg of tissue for fluorescence. Bars represent mean ± SEM of 3–10 animals. Significant differences between means were analyzed using one-way ANOVA followed by Bonferroni as a posterio test ***$p < 0.001$ versus basal levels, †$p < 0.05$; †††$P < 0.001$ versus NADPH-stimulated, ##$p < 0.01$ versus LZR. (c–f) Average inhibitory effect of the Nox1/4 GKT137831 inhibitor (0.3 μM) (c,d) and the non-selective Nox4 inhibitor plumbagin (1 μM) (e,f) on the relaxations induced by the endothelial agonist ACh under conditions of NOS and COX blockade (100 μM L-NOARG and 0.3 μM indomethacin) in renal arteries of LZR (c,e) and OZR (d,f). Data are shown as the mean ± SEM of 6–13 arteries from 7 animals. Significant differences were analyzed using Student t-test for paired observations *$p < 0.05$; **$p < 0.01$ versus control before treatment.

significantly reduced by the selective Nox1 inhibitor NoxA1ds (Fig. 10a), and also H_2O_2 levels of LZR and to a lesser extent those of OZR (Fig. 10b). The effect of the selective Nox1 inhibitor was further evaluated on the relaxant responses to the endothelial agonist ACh under conditions NOS and COX blockade. NoxA1ds hardly affected ACh-elicited relaxations in LZR (Fig. 10c) and those in OZR (Fig. 10d), thus ruling out a major role of Nox1-derived H_2O_2 in the endothelium-dependent vasodilation of renal arteries. However, in the absence of L-NOARG to inhibit eNOS and NO formation, selective inhibition of Nox1 with NoxA1ds significantly improved impaired ACh endothelial relaxations in OZR thus suggesting that Nox1-derived $O_2^{\cdot-}$ contributes to renal endothelial dysfunction in obesity.

4. Discussion

Oxidative stress has been implicated in the pathogenesis of diabetes and obesity-related microvascular complications including kidney injury [1,2,30]. The major findings of the present study are that augmented Nox-derived $O_2^{\cdot-}$ is involved in kidney vascular oxidative stress and endothelial dysfunction in obesity but there is a differential contribution of the various Nox members of the NADPH oxidase family. While Nox1 and Nox2 were up-regulated in renal arteries and contributed to the increased $O_2^{\cdot-}$ generation and endothelial dysfunction, reduced endothelial Nox4 expression was associated with decreased Nox-derived H_2O_2 and impaired H_2O_2–mediated vasodilatation which might hinder Nox protective renal vascular effects and thus indirectly promote impaired endothelial function.

Renal inflammation and oxidative stress have earlier been found along with endothelial dysfunction in renal arterioles of genetic and HFD models of obesity [18,23], and initially ascribed to up-regulation of COX-2 that contributed to plasma and renal oxidative stress and augmented vasoconstriction [23,31]. The present data confirm endothelial dysfunction in renal interlobar arterioles of genetically obese rats, as depicted by the impaired ACh-induced relaxations; however, antioxidant treatment including non-selective Nox inhibition hardly ameliorated impaired ACh relaxant responses despite augmented basal and ET-1-stimulated $O_2^{\cdot-}$ levels in the arterial wall, that have been reported to greatly contribute to vascular oxidative stress and reduced endothelial NO bioavailability in obesity [27]. A substantial fraction of the endothelium-dependent responses of renal arterioles is mediated by a non-NO non-prostanoid relaxing factor and is associated with VSM hyperpolarization [32,33]. When pharmacologically dissecting the components of the relaxant responses of renal arteries in OZR, we found that enhanced non-NO non-prostanoid EDH type relaxations compensated for impaired NO-mediated responses of renal arteries in obese rats, as depicted by the lesser reduction of these relaxations by NOS inhibition in OZR, but the larger relaxant responses unmasked upon blockade of NO and prostanoid synthesis. This increased contribution of EDH-type responses to counteract diminished NO bioavailability is consistent with that recently shown in coronary, mesenteric and subcutaneous arteries from diabetic rats and patients [34–36], and ascribed to the enhanced activity of endothelial K_{Ca} channels [35]. On the other hand, impaired NO-mediated endothelial dysfunction found for renal interlobar arteries of obese rats would also be expected to occur in afferent arterioles, wherein the relative contribution of NO and non-NO non prostanoid EDH-type factors has earlier been reported to be similar to that found for the preglomerular arteries in the present study [33].

H_2O_2 derived from both CYP 2C epoxygenases and Nox contributes to the EDH-type responses in healthy renal arteries [4,37], which might explain the lack of significant effect of ROS scavengers on endothelial relaxations of OZR despite augmented arterial oxidative stress. However, the enhanced EDH-type relaxant responses observed in renal arteries from obese rats cannot be ascribed to a larger contribution of H_2O_2 to these responses since they were not further inhibited by catalase. Moreover, NADPH-dependent H_2O_2 generation was reduced in both renal arteries and cortex of OZR compared to lean controls despite the overall NADPH-dependent $O_2^{\cdot-}$ production was enhanced in kidney tissues, in particular in intrarenal arteries. Diminished H_2O_2 levels cannot either be due to reduced antioxidant H_2O_2-generating enzymes CuZnSOD and MnSOD, since they were up-regulated in both renal arteries and cortex, in particular the mitochondrial SOD isoform whose expression was markedly enhanced in vascular tissue including renal arterioles and glomeruli. Interestingly, these results are in line with those recently reported for the diabetic kidney wherein reduced mitochondrial H_2O_2 generation measured with Amplex Red was observed despite the enhanced overall kidney ROS production, suggesting an

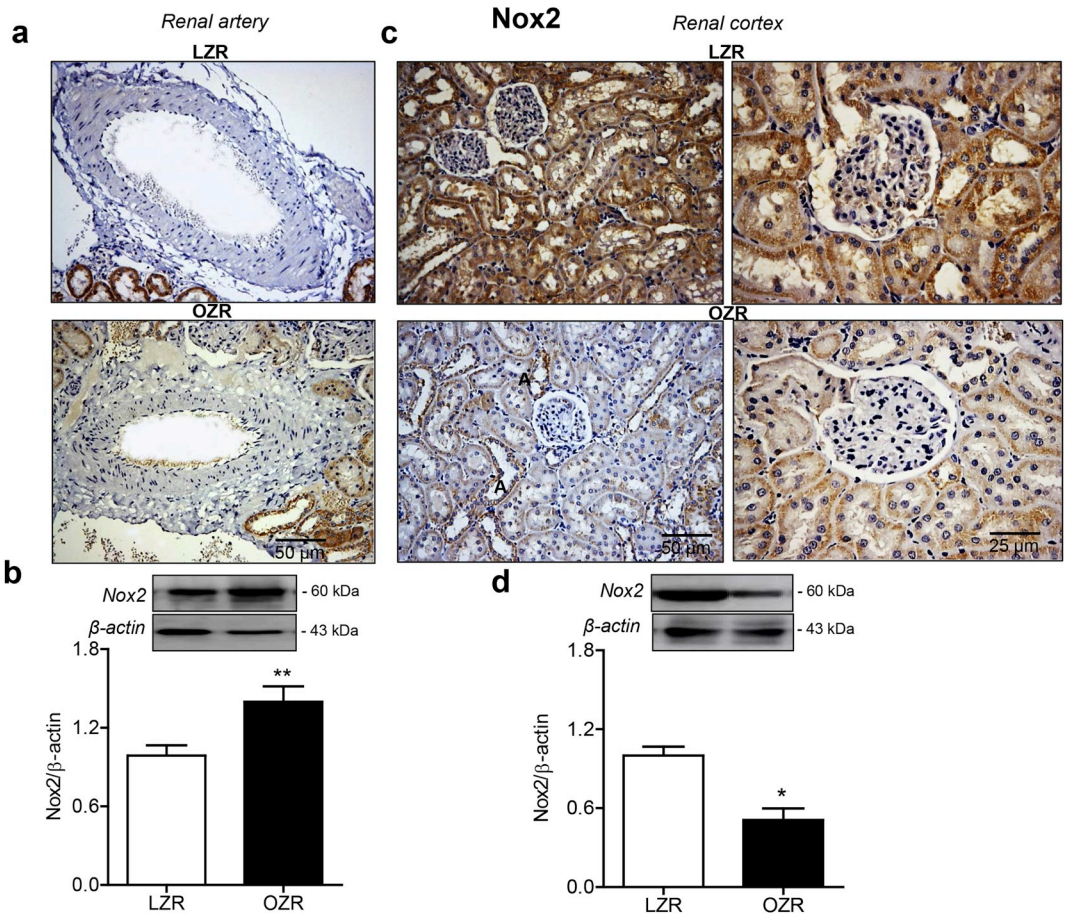

Fig. 7. Nox2 is up-regulated in renal arteries but down-regulated in renal cortex of obese rats. (a,c) Inmunohistochemical demostration of Nox2 in renal interlobar artery (a) and cortex (c) from rat kidney of LZR and OZR. Nox2 protein was distributed throughout the arterial wall in arteries and arterioles (A) with a high density in renal tubules of LZR that was markedly reduced in OZR (c). Scale bars indicate 50 μm and 25 μm. Sections are representative of n = 3 animals. (b) Western blot analysis of Nox2 expression in samples of renal artery and cortex showing that Nox2 protein levels were higher in renal arteries (b) but downregulated in samples of renal cortex from OZR (d) compared to LZR. Results were quantified by densitometry and presented as a ratio of density of Nox2 band vs those of β-actin from the sample. Data are shown as the mean ± SEM of 4 animals. Significant differences were analyzed using unpaired *t*-test *p < 0.05; **p < 0.01 versus LZR.

impaired mitochondrial activity that was ascribed to AMPK dysregulation [2,38]. Interestingly, in our study a reduced expression of Nox4, mostly restricted to endothelial cells in healthy arteries [4], was also found along with the diminished NADPH-dependent H_2O_2 generation in renal arteries of obese rats suggesting that down-regulation of this Nox subunit might be involved in the lower levels of arterial H_2O_2. Moreover, Nox4-derived H_2O_2 production measured with Amplex Red and to a lesser extent its contribution to the EDH-type endothelial relaxations of renal arterioles from OZR were also significantly reduced, as depicted by the lower inhibitory effect of the Nox inhibitors GKT137831 and plumbagin on these responses compared to that on arteries from lean rats. Thus, in contrast to Nox1 or Nox2 that primarily produce $O_2^{\cdot-}$, Nox4 produces H_2O_2 rather than $O_2^{\cdot-}$ [39] and has been identified as a functional source of ROS generation in the mitochondria of kidney cortex, wherein the mitochondrial SOD effectively dismutates Nox4-derived superoxide to H_2O_2 [40]. Moreover, mitochondria-derived H_2O_2 has recently been shown to effectively contribute to the EDH-type endothelium-dependent relaxations of renal small arteries [4].

Down-regulation of arterial Nox4 expression and reduced Nox4-derived H_2O_2 production in genetically obese rats contrast with studies linking Nox4 to renal pathology and showing that genetic deficiency or pharmacological inhibition of Nox4 ameliorated enhanced Nox4-derived ROS generation, glomerular injury and kidney inflammation and fibrosis in diabetic mice [6,7]. However, our results showing lower levels of vascular Nox4 coupled to impaired Nox4-derived H_2O_2 generation would be consistent with the reduced expression of tubular Nox4 and H_2O_2 generation found in hyperglycemic type I diabetic mice and in other models of chronic kidney disease, as well as with the worsening of renal function and fibrosis upon genetic deletion of Nox4 in diabetic models, which suggests a protective role of Nox4 in renal disease [9,10]. The protective role of endothelial Nox4 as a source of vasodilator H_2O_2 in renal arteries recently shown by us is also confirmed in our study, but the impact of reduced Nox4-derived endothelial H_2O_2 generation in renal endothelial function of obese rats is difficult to assess due to the non-NO non-prostanoid EDH-type mechanisms that compensate for the diminished NO bioavalability and impaired endothelial vasodilatation [34–36].

Nox2 and Nox1 have been linked to endothelial and vascular dysfunction in metabolic disease and hypertension [41–45], and both Nox subunits, in particular Nox2, are closely related to vascular inflammation [41]. Many metabolic and cardiovascular disorders including insulin resistance, obesity and atherosclerosis exhibit a chronic low-grade inflammation at the vascular wall and are associated with the redox-sensitive NF-κB inflammatory signaling pathway activated by Nox-derived ROS in response to high levels of glucose, LDL cholesterol and free fatty acid (FFA) stimulation [41]. Since obesity is usually related to other metabolic and vascular disorders such as insulin resistance, dyslipidaemia, impaired glucose tolerance and hypertension, jointly referred to as the metabolic syndrome [46], dyslipidemia (hypertriglyceridemia and hypercholesterolemia) and insulin resistance of the obese Zucker rat used in the present study could in fact account for the marked up-regulation of pro-inflammatory Nox2 and Nox1 subunits

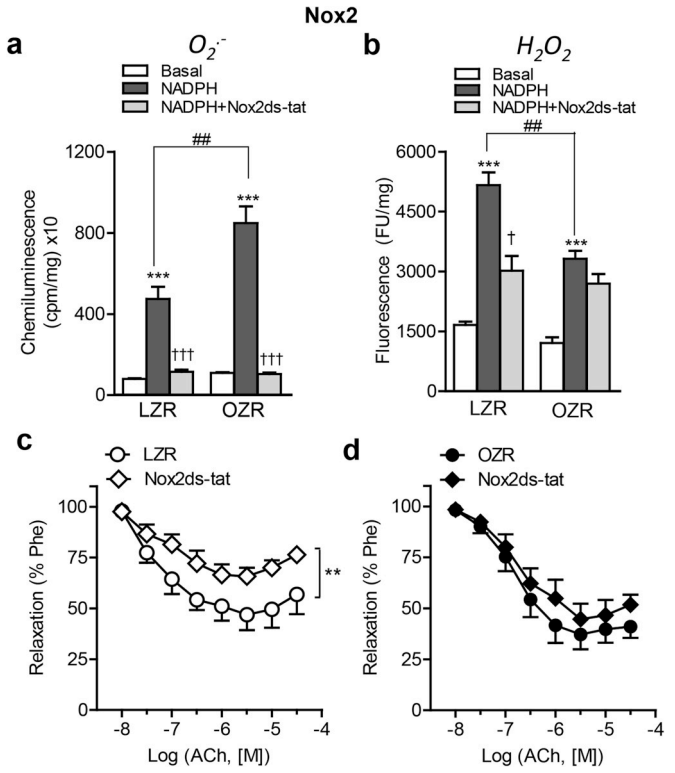

Fig. 8. Blockade of Nox2 reduces $O_2^{\cdot-}$ generation but does not further inhibit H_2O_2-mediated renal endothelium-dependent relaxations of obese rats. (a,b) Effect of the selective Nox2 inhibitor Nox2ds-tat (1 μM) on the NADPH-stimulated levels of $O_2^{\cdot-}$ (a) and H_2O_2 (b) measured by lucigenin-enhanced chemiluminescence and by Amplex Red fluorescence, respectively, in renal arteries of LZR and OZR. Results are expressed in counts per minute (cpm) per mg of tissue for chemiluminescence and in relative fluorescence units (RFU) per mg of tissue for fluorescence. Bars represent mean ± SEM of 3–10 animals. Significant differences between means were analyzed using one-way ANOVA followed by Bonferroni as a posterio test ***p < 0.001 versus basal levels, †p < 0.05; †††P < 0.001 versus NADPH-stimulated, ##p < 0.01 versus LZR. (c,d) Average inhibitory effect of the Nox2 inhibitor Nox2ds-tat (1 μM) on the relaxations induced by the endothelial agonist ACh under conditions of NOS and COX blockade (100 μM L-NOARG and 0.3 μM indomethacin) in renal arteries of LZR (c) and OZR (d). Data are shown as the mean ± SEM of 6–12 arteries from 6 animals. Significant differences were analyzed using paired Student t-test **p < 0.01 versus control before treatment.

and enhanced Nox-derived oxidative stress found in renal arteries of obese animals [41,46,47]. Expression of Nox2 (gp91phox), the classic NADPH oxidase primarily found in phagocytic cells, followed different trends in kidney cortex and renal arterioles of obese rats. Thus, whereas Nox2 was up-regulated in renal arteries, its expression was markedly reduced in renal cortex of OZR. Up-regulation of arterial Nox2 was associated with enhanced ROS-generating Nox2 activity as shown by the larger PKC-activated and NADPH-dependent $O_2^{\cdot-}$ production sensitive to the selective Nox2 inhibitor Nos2ds-tat. These findings are consistent with those reported in aorta [47] and cerebral arteries [48] from HFD-fed insulin resistant hyperlipidemic obese mice showing that endothelial Nox2-derived superoxide played a major role in endothelial dysfunction, while Nox2-deficiency or Nox2 pharmacological blockade was protective from vascular oxidative stress, impaired endothelial insulin Akt-eNOS-NO pathway and endothelial dysfunction [47]. The specific relationship between insulin resistance and vascular Nox2-derived oxidative stress has been demonstrated in insulin-resistant endothelial cells wherein enhanced $O_2^{\cdot-}$ production was selectively inhibited by gp91ds-tat or siRNA-mediated knockdown of Nox2, while insulin-resistance-induced impaired endothelium-dependent vasodilation and vascular function was improved by Nox2 deletion [49], Moreover, ex vivo exposure to insulin reduced flow-induced vasodilatation and NO formation and increased ROS production in human skeletal muscle arterioles, these insulin effects being reversed by Nox2 inhibitors [50]. In the latter study, hypersinsulinemia increased Nox2 but not Nox4 expression and activity thus augmenting $O_2^{\cdot-}$ generation in microvascular endothelial cells from adipose tissue, which reduces NO availability and enhances peroxynitrite formation [50]. In our study, while $O_2^{\cdot-}$, was enhanced Nox2-derived H_2O_2 levels were significantly reduced in renal arteries from OZR compared to lean rats, and so were the Nox2-dependent H_2O_2-mediated endothelium dependent relaxations. Endothelial H_2O_2 derived from both Nox4 and Nox2 contributes to the endothelium-dependent relaxations of healthy renal arteries [4], and the present data demonstrate that this contribution is impaired in obesity therefore hindering Nox protective effects on renal endothelial function.

Interestingly, in contrast to the enhanced expression of Nox2 in renal arteries, Nox2 was markedly down-regulated in kidney cortex, specifically in renal tubules of obese rats, in agreement with that earlier found in leptin receptor-deficient hyperglycemic db/db mice wherein both Nox2 gen and protein expression were reduced in renal cortex [6]. In the latter rodent model of type II diabetes and obesity, down-regulation of Nox2 was interpreted as a compensatory mechanism to counterregulate the enhanced Nox4/p22phox expression, augmented ROS generation and activation of redox-sensitive profibrotic and proinflammatory pathways being ascribed to Nox4 [6]. However, in our study the whole Nox4 subunit content was unchanged in kidney cortex and markedly reduced in renal arteries of insulin resistant OZR. On the other hand, studies in Nox2-deficient mice have further demonstrated that the lack of Nox2 does not protect against oxidative stress, glomerular hypertrophy and fibrosis in diabetic kidney disease, the latter being again ascribed to up-regulation of Nox4 [12]. In fact, Nox2-derived superoxide is involved in several renal tubular functions, such as regulation of tubuloglomerular feedback and macula densa responses to high salt [51] and potassium transport in the collecting duct [52]. Therefore, taken together, the present data along with those reported in the kidney of rodent models of type 2 diabetes showing decreased expression of Nox2 gene and protein [6] suggest that loss of Nox2-mediated renal tubular functions might contribute to diabetes and obesity-associated kidney injury.

Unlike Nox2 and Nox4 members of the NADPH oxidase family, whose expression was either unchanged or downregulated in renal cortex of insulin resistant obese rats, Nox1 was marked and uniformly enhanced in renal cortex of OZR which supports earlier findings in glomeruli of type 1 diabetic mice [53] and cortex of HFD-fed rats [17]. In these studies, Nox1-derived oxidative stress was associated with inflammation, podocyte injury and albuminuria, and treatment with the SOD mimetic tempol improved metabolic profile and ameliorated kidney injury and renal dysfunction [17], thus suggesting a main role of Nox1 in diabetic and obesity nephropathy. In our study, Nox1 was mostly found in arterioles and renal tubule epithelium of renal cortex, the latter supporting earlier studies showing that Nox1 is highly expressed in the intestinal epithelium in response to transcriptional up-regulation of its promoter by cytokines involved in host defense [41,54]. Many of the renoprotective effects on diabetic nephropathy reported for the Nox1/Nox4 inhibitor and ascribed to Nox4 could therefore be also due to Nox1 [7,11,55].

Nox1 is a major source of $O_2^{\cdot-}$ generation in endothelial cells, VSM cells and fibroblasts under both physiological and pathophysiological conditions. This Nox subunit participates in shear-induced outwards vascular remodelling, while in vascular pathology it has primarily been involved in hypertension and proliferative vascular disease [41]. Both Nox2 and Nox4, but not Nox1 are expressed in human and rat intrarenal arteries [4,56]. In the present study, a low expression of Nox1 was found in renal arteries of lean rats, but obesity induced a marked up-regulation of this subunit in VSM of both interlobar arteries and cortical arterioles. Recent studies have identified Nox1 as a critical

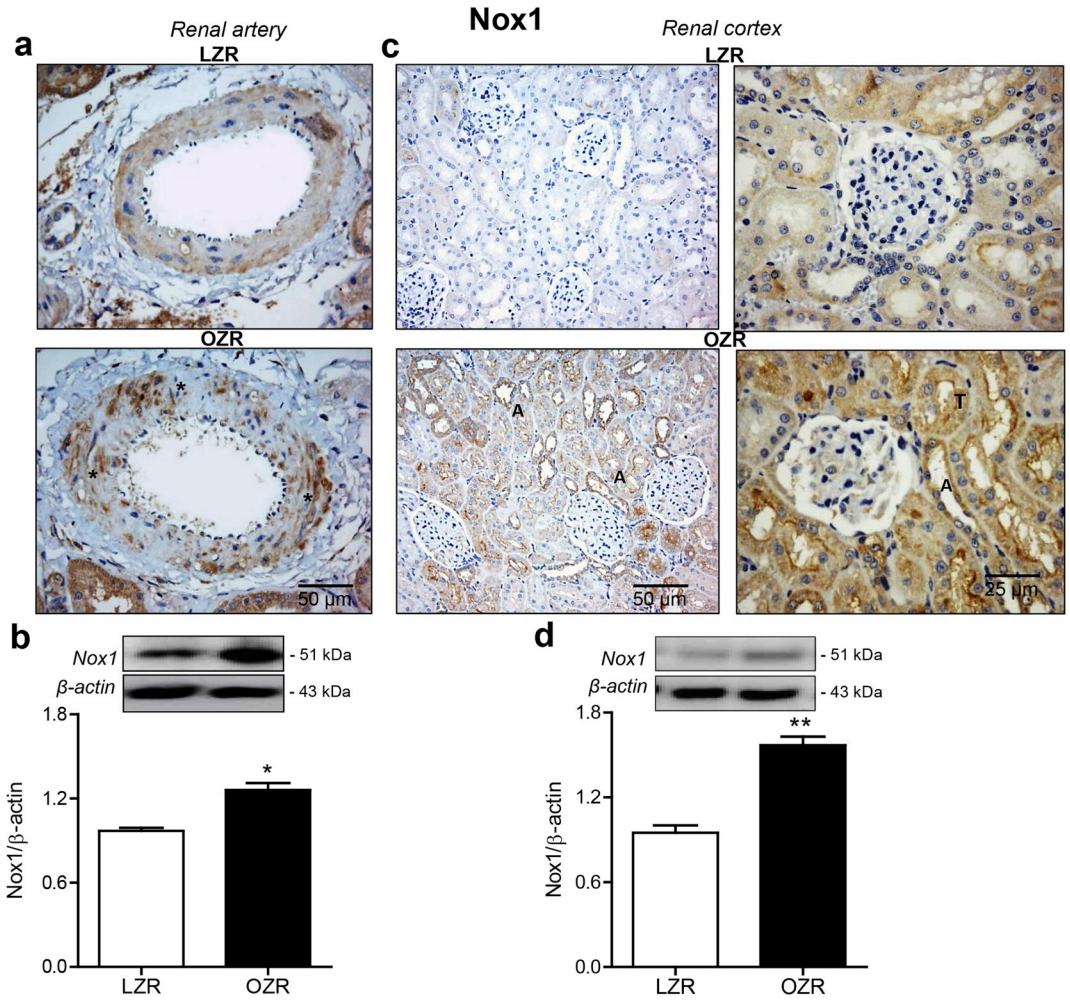

Fig. 9. Nox1 is up-regulated in renal arteries and cortex of obese rats. (a,c) Inmunohistochemical demostration of Nox1 in renal interlobar artery and cortex from LZR and OZR kidney. (a,c) Nox1 protein was scarcely distributed in renal interlobar artery, mainly in VSM (*) (a) with a very low density in renal cortex (c) of LZR. In OZR, density of Nox1 protein was markedly enhanced in VSM of interlobar arteries (a) and in arterioles (A), glomeruli and renal tubule (T) epithelium of renal cortex (c). Scale bars indicate 50 μm and 25 μm. Sections are representative of n = 3 animals. (b) Western blot analysis of Nox1 expression in samples of renal artery and cortex showing that Nox1 protein levels were higher in samples of both renal arteries (b) and renal cortex (d) from OZR compared to LZR. Results were quantified by densitometry and presented as a ratio of density of Nox1 band vs those of β-actin from the sample. Data are shown as the mean ± SEM of 4 animals. Significant differences were analyzed using unpaired *t*-test *p < 0.05; **p < 0.01 versus LZR.

source of ROS responsible for microvascular dysfunction in metabolic disease, and deletion of Nox1 [29] or the Nox1 organizer NoxO1 [45] abolished oxidative stress and improved endothelial dysfunction and VSM dilation in mesenteric microvessels of diabetic mice, and attenuated atherosclerosis development in diabetes mellitus [41,55]. The present data support the involvement of Nox1 in kidney vascular oxidative stress in obesity, since both $O_2^{\cdot-}$ and H_2O_2 production were abolished by the selective Nox1 inhibitor NoxA1ds in renal arterioles of OZR. On the other hand, in contrast to Nox2 and Nox4 [4], Nox1 does not seem to be a relevant physiological source of vasodilator H_2O_2, since Nox1ds did not significantly attenuate non-NO non-prostanoid endothelial relaxations of intrarenal arteries in LZR, although it had a moderate inhibitory effect of these responses in obese rats, possibly due to up-regulation of VSM CuZnSOD activity that dismutates augmented Nox1-derived $O_2^{\cdot-}$ to H_2O_2 in renal arteries.

In the present study, up-regulation of Nox1 was particularly evident in VSM of obese rats. Overexpression of VSM Nox1 leading to enhanced production of ROS in response to angiotensin II causes eNOS uncoupling and decreases NO bioavailability resulting in impaired vasorelaxation thus showing a crosstalk between Nox1 up-regulation in VSM and endothelial function [57]. Moreover, NoxO1 and p47phox-dependent activation of Nox1, but not that of Nox2, Nox4 or mitochondrion, mediates eNOS uncoupling and endothelial dysfunction in type I diabetic mice [58]. Augmented basal oxidative stress in renal interlobar arteries of obese rats is in part due to eNOS uncoupling and reduced by NOS blockade [23]. The present data show that the absence of NOS blockade unmasked a beneficial effect of the selective Nox1 inhibitor NoxA1ds on the impaired NO-mediated relaxations of renal arteries of genetically obese rats. This improvement was not observed with apocynin, a general Nox inhibitor with higher affinity for Nox2, which suggests that Nox1-derived $O_2^{\cdot-}$ mostly derived of VSM impairs NO-mediated endothelium-dependent responses and is therefore involved in renal endothelial dysfunction in obesity.

In conclusion, the present study provides novel data on the differential contribution of Nox subunits from the NADPH family to kidney vascular oxidative stress and endothelial dysfunction in obesity. Nox4, considered to play a key role in the pathogenesis of diabetic nephropathy, is down-regulated in the renal endothelium of obese rats and the contribution of Nox4-derived H_2O_2 to renal endothelial vasodilation is impaired, thus hindering Nox4 protective vascular effects. In contrast, Nox1 is uniformly up-regulated in both arterial and renal cortex tissues of obese rats and Nox1-derived $O_2^{\cdot-}$ underlies endothelial dysfunction, which suggests that this specific Nox subunit might be critical in the development of obesity-associated microvascular complications. In this

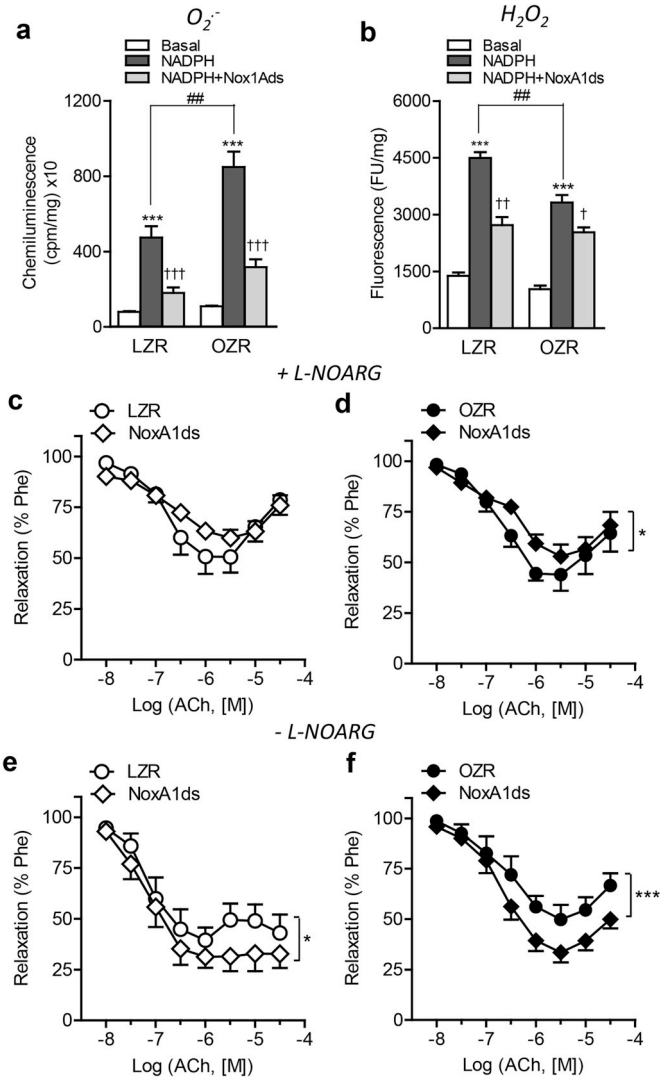

Fig. 10. Blockade of Nox1 reduces $O_2^{\cdot-}$ generation and improves renal endothelium-dependent relaxations in the absence of NOS blockade in obese rats. (a,b) Effect of the selective Nox1 inhibitor NoxA1ds (0.3 μM) on the NADPH-stimulated levels of $O_2^{\cdot-}$ (a) and H_2O_2 (b) production measured by lucigenin-enhanced chemiluminescence and by Amplex Red fluorescence, respectively, in renal arteries from rat kidney of LZR and OZR. Results are expressed in counts per minute (cpm) per mg of tissue for chemiluminescence and in relative fluorescence units (RFU) per mg of tissue for fluorescence. Bars represent mean ± SEM of 2–10 animals. Significant differences between means were analyzed using one-way ANOVA followed by Bonferroni as a posterio test ***p < 0.001 versus basal levels, †p < 0.05, ††p < 0.01; †††P < 0.001 versus NADPH-stimulated, ##p < 0.01 versus LZR. (c–f) Average inhibitory effect of the Nox1 inhibitor NoxA1ds (0.3 μM) on the relaxations induced by the endothelial agonist ACh in renal arteries of LZR (c,e) and OZR (d,f), in the absence (e,f) and the presence (c,d) of L-NOARG (100 μM) and indomethacin (0.3 μM). Data are shown as the mean ± SEM of 8–11 arteries from 6 animals. Significant differences were analyzed using paired *t*-test **p < 0.01 versus control before treatment.

respect, renoprotective effects earlier reported for Nox1/Nox4 inhibitors in metabolic disease and ascribed to reduction of Nox4-mediated effects might have indeed been due to Nox1 inhibition, and the use of selective Nox1 inhibitors may be beneficial to prevent endothelial and vascular dysfunction in obesity-related nephropathy.

Sources of support

This work was supported by grant SAF2016-77526R from Ministerio de Economia y Competitividad (MINECO,Spain)-Fondo Europeo de Desarrollo Regional (FEDER).

Conflicts of interest

All the authors declare no conflicts of interest.

Acknowledgements

We thank Francisco Puente and Manuel Perales for their expert technical assistance.

Appendix A. Supplementary data

Supplementary data to this article can be found online at https://doi.org/10.1016/j.redox.2019.101330.

References

[1] J.M. Forbes, M.T. Coughlan, M.E. Cooper, Oxidative stress as a major culprit in kidney disease in diabetes, Diabetes 57 (2008) 1446–1454.
[2] K. Sharma, Obesity and diabetic kidney disease: role of oxidant stress and redox balance, Antioxidants Redox Signal. 25 (2016) 208–216.
[3] M. Sedeek, R. Nasrallah, R.M. Touyz, R.L. Hébert, NADPH oxidases, reactive oxygen species, and the kidney: friend and foe, J. Am. Soc. Nephrol. 24 (2013) 1512–1518.
[4] M. Muñoz, M.P. Martínez, M.E. López-Oliva, C. Rodríguez, C. Corbacho, J. Carballido, A. García-Sacristán, M. Hernández, L. Rivera, J. Sáenz-Medina, D. Prieto, Hydrogen peroxide derived from NADPH oxidase 4- and 2 contributes to the endothelium-dependent vasodilatation of intrarenal arteries, Redox Biol 19 (2018) 92–104.
[5] Y. Gorin, K. Block, J. Hernandez, B. Bhandari, B. Wagner, J.L. Barnes, H.E. Abboud, Nox4 NAD(P)H oxidase mediates hypertrophy and fibronectin expression in the diabetic kidney, J. Biol. Chem. 280 (2005) 39616–39626.
[6] M. Sedeek, G. Callera, A. Montezano, A. Gutsol, F. Heitz, C. Szyndralewiez, P. Page, C.R. Kennedy, K.D. Burns, R.M. Touyz, R.L. Hébert, Critical role of Nox4-based NADPH oxidase in glucose-induced oxidative stress in the kidney: implications in type 2 diabetic nephropathy, Am. J. Physiol. Renal. Physiol. 299 (2010) F1348–F1358.
[7] J.C. Jha, S.P. Gray, D. Barit, J. Okabe, A. El-Osta, T. Namikoshi, V. Thallas-Bonke, K. Wingler, C. Szyndralewiez, F. Heitz, R.M. Touyz, M.E. Cooper, H.H. Schmidt, K.A. Jandeleit-Dahm, Genetic targeting or pharmacologic inhibition of NADPH oxidase nox4 provides renoprotection in long-term diabetic nephropathy, J. Am. Soc. Nephrol. 25 (2014) 1237–1254.
[8] Y.H. You, T. Quach, R. Saito, J. Pham, K. Sharma, Metabolomics reveals a key role for fumarate in mediating the effects of NADPH oxidase 4 in diabetic kidney disease, J. Am. Soc. Nephrol. 27 (2016) 466–481.
[9] A. Babelova, D. Avaniadi, O. Jung, C. Fork, J. Beckmann, J. Kosowski, N. Weissmann, N. Anilkumar, A.M. Shah, L. Schaefer, K. Schröder, R.P. Brandes, Role of Nox4 in murine models of kidney disease, Free Radic. Biol. Med. 53 (2012) 842–853.
[10] S. Nlandu Khodo, E. Dizin, G. Sossauer, I. Szanto, P.Y. Martin, E. Feraille, K.H. Krause, S. de Seigneux, NADPH-oxidase 4 protects against kidney fibrosis during chronic renal injury, J. Am. Soc. Nephrol. 23 (2012) 1967–1976.
[11] M. Sedeek, A. Gutsol, A.C. Montezano, D. Burger, A. Nguyen Dinh Cat, C.R. Kennedy, K.D. Burns, M.E. Cooper, K. Jandeleit-Dahm, P. Page, C. Szyndralewiez, F. Heitz, R.L. Hebert, R.M. Touyz, Renoprotective effects of a novel Nox1/4 inhibitor in a mouse model of Type 2 diabetes, Clin. Sci. 124 (2013) 191–202.
[12] Y.H. You, S. Okada, S. Ly, K. Jandeleit-Dahm, D. Barit, T. Namikoshi, K. Sharma, Role of Nox2 in diabetic kidney disease, Am. J. Physiol. Renal. Physiol. 304 (2013) F840–F848.
[13] H. Kramer, A. Luke, A. Bidani, G. Cao, R. Cooper, D. McGee, Obesity and prevalent and incident CKD: the hypertension detection and follow-up program, Am. J. Kidney Dis. 46 (2005) 587–594.
[14] A.P. de Vries, P. Ruggenenti, X.Z. Ruan, M. Praga, J.M. Cruzado, I.M. Bajema, V.D. D'Agati, H.J. Lamb, D. Pongrac Barlovic, R. Hojs, M. Abbate, R. Rodriquez, C.E. Mogensen, E. Porrini, Fatty kidney: emerging role of ectopic lipid in obesity-related renal disease, Lancet Diabetes Endocrinol 2 (2014) 417–426.
[15] K.A. Griffin, H. Kramer, A.K. Bidani, Adverse renal consequences of obesity, Am. J. Physiol. Renal. Physiol. 294 (2008) F685–F696.
[16] A.V. Mathew, S. Okada, K. Sharma, Obesity related kidney disease, Diabetes 7 (2011) 41–49.
[17] P.J. Ebenezer, N. Mariappan, C.M. Elks, M. Haque, J. Francis, Diet-induced renal changes in Zucker rats are ameliorated by the superoxide dismutase mimetic TEMPOL, Obesity 17 (2009) 1994–2002.
[18] A.A. Elmarakby, J.D. Imig, Obesity is the major contributor to vascular dysfunction and inflammation in high-fat diet hypertensive rats, Clin. Sci. 118 (2010) 291–301.
[19] B.B. Ratliff, W. Abdulmahdi, R. Pawar, M.S. Wolin, Oxidant mechanisms in renal injury and disease, Antioxidants Redox Signal. 25 (2016) 119–146.
[20] C. Ruggiero, M. Ehrenshaft, E. Cleland, K. Stadler, High-fat diet induces an initial

adaptation of mitochondrial bioenergetics in the kidney despite evident oxidative stress and mitochondrial ROS production, Am. J. Physiol. Endocrinol. Metab. 300 (2011) E1047–E1058.
[21] H.H. Szeto, S. Liu, Y. Soong, N. Alam, G.T. Prusky, S.V. Seshan, Protection of mitochondria prevents high-fat diet-induced glomerulopathy and proximal tubular injury, Kidney Int. 90 (2016) 997–1011.
[22] A.E. Declèves, Z. Zolkipli, J. Satriano, L. Wang, T. Nakayama, M. Rogac, T.P. Le, J.L. Nortier, M.G. Farquhar, R.K. Naviaux, K. Sharma, Regulation of lipid accumulation by AMP-activated kinase [corrected] in high fat diet-induced kidney injury, Kidney Int. 85 (2014) 611–623.
[23] M. Muñoz, A. Sánchez, M.P. Martínez, S. Benedito, M.E. López-Oliva, A. García-Sacristán, M. Hernández, D. Prieto, COX-2 is involved in vascular oxidative stress and endothelial dysfunction of renal interlobar arteries from obese Zucker rats, Free Radic. Biol. Med. 84 (2015) 77–90.
[24] B.L. Kasiske, M.P. Cleary, M.P. O'Donnell, W.F. Keane, Effects of genetic obesity on renal structure and function in the Zucker rat, J. Lab. Clin. Med. 106 (1985) 598–604.
[25] T.M. Coimbra, U. Janssen, H.J. Gröne, T. Ostendorf, U. Kunter, H. Schmidt, G. Brabant, J. Floege, Early events leading to renal injury in obese Zucker (fatty) rats with type II diabetes, Kidney Int. 57 (2000) 167–182.
[26] D.J. Ranayhossaini, A.L. Rodriguez, S. Sahoo, B.B. Chen, R.K. Mallampalli, E.E. Kelley, G. Csany, M.T. Gladwin, G. Romero, P.J. Pagano, Selective recapitulation of conserved and nonconserved regions of putative NOXA1 protein activation domain confers isoform-specific inhibition of Nox1 oxidase and attenuation of endothelial cell migration, J. Biol. Chem. 288 (2013) 36437–36450 288.
[27] A. Sánchez A, P. Martínez, M. Muñoz M, S. Benedito, A. García-Sacristán, M. Hernández, D. Prieto, Endothelin-1 contributes to endothelial dysfunction and enhanced vasoconstriction through augmented superoxide production in penile arteries from insulin-resistant obese rats: role of ET(A) and ET(B) receptors, Br. J. Pharmacol. 171 (2014) 5682–5695.
[28] S. Selemidis, C.G. Sobey, K. Wingler, H.H. Schmidt, G.R. Drummond, NADPH oxidases in the vasculature: molecular features, roles in disease and pharmacological inhibition, Pharmacol. Ther. 120 (2008) 254–291.
[29] J.A. Thompson, S. Larion, J.D. Mintz, E.J. Belin de Chantemèle, D.J. Fulton, D.W. Stepp, Genetic deletion of NADPH oxidase 1 rescues microvascular function in mice with metabolic disease, Circ. Res. 121 (2017) 502–511.
[30] D. Prieto, C. Contreras, A. Sánchez, Endothelial dysfunction, obesity and insulin resistance, Curr. Vasc. Pharmacol. 12 (2014) 412–426.
[31] A. Dey, C. Maric, W.H. Kaesemeyer, C.Z. Zaharis, J. Stewart, J.S. Pollock, J.D. Imig, Rofecoxib decreases renal injury in obese Zucker rats, Clin. Sci. 107 (2004) 561–570.
[32] E. Büssemaker, R. Popp, J. Binder, R. Busse, I. Fleming, Characterization of the endothelium-derived hyperpolarizing factor (EDHF) response in the human interlobar artery, Kidney Int. 63 (2003) 1749–1755.
[33] D. Wang, L.J. Borrego-Conde, J.R. Falck, K.K. Sharma, C.S. Wilcox, J.G. Umans, Contributions of nitric oxide, EDHF, and EETs to endothelium-dependent relaxation in renal afferent arterioles, Kidney Int. 63 (2003) 2187–2193.
[34] S.S. Mokhtar, P.M. Vanhoutte, S.W. Leung, M.I. Yusof, W.A. Wan Sulaiman, A.Z. Mat Saad, R. Suppian, A.H. Rasool, Endothelium dependent hyperpolarization-type relaxation compensates for attenuated nitric oxide-mediated responses in subcutaneous arteries of diabetic patients, Nitric Oxide 53 (2016) 35–44.
[35] C. Schach, M. Resch, P.M. Schmid, G.A. Riegger, D.H. Endemann, Type 2 diabetes: increased expression and contribution of IKCa channels to vasodilation in small mesenteric arteries of ZDF rats, Am. J. Physiol. Heart Circ. Physiol. 307 (2014) H1093–H1102.
[36] T. Yada, H. Shimokawa, H. Tachibana, Endothelium-dependent hyperpolarization-mediated vasodilatation compensates nitric oxide-mediated endothelial dysfunction during ischemia in diabetes-induced canine coronary collateral microcirculation in vivo, Microcirculation 25 (2018) e12456.
[37] M. Muñoz, M.E. López-Oliva, E. Pinilla, M.P. Martínez, A. Sánchez, C. Rodríguez, A. García-Sacristán, M. Hernández, L. Rivera, D. Prieto, CYP epoxygenase-derived H2O2 is involved in the endothelium-derived hyperpolarization (EDH) and relaxation of intrarenal arteries, Free Radic. Biol. Med. 106 (2017) 168–183.
[38] L.L. Dugan, Y.H. You, S.S. Ali, M. Diamond-Stanic, S. Miyamoto, A.E. DeCleves, A. Andreyev, T. Quach, S. Ly, G. Shekhtman, W. Nguyen, A. Chepetan, T.P. Le, L. Wang, M. Xu, K.P. Paik, A. Fogo, B. Viollet, A. Murphy, F. Brosius, R.K. Naviaux, K. Sharma, AMPK dysregulation promotes diabetes-related reduction of superoxide and mitochondrial function, J. Clin. Investig. 123 (2013) 4888–4899.
[39] I. Takac, K. Schröder, L. Zhang, B. Lardy, N. Anilkumar, J.D. Lambeth, A.M. Shah, F. Morel, R.P. Brandes, The E-loop is involved in hydrogen peroxide formation by the NADPH oxidase Nox4, J. Biol. Chem. 286 (2011) 13304–13313.
[40] K. Block, Y. Gorin, H.E. Abboud, Subcellular localization of Nox4 and regulation in diabetes, Proc. Natl. Acad. Sci. U. S. A. 106 (2009) 14385–14390.
[41] S.J. Forrester, D.S. Kikuchi, M.S. Hernandes, Q. Xu, K.K. Griendling, Reactive oxygen species in metabolic and inflammatory signaling, Circ. Res. 122 (2018) 877–902.
[42] S. Wind, K. Beuerlein, M.E. Armitage, A. Taye, A.H. Kumar, D. Janowitz, C. Neff, A.M. Shah, K. Wingler, H.H. Schmidt, Oxidative stress and endothelial dysfunction in aortas of aged spontaneously hypertensive rats by NOX1/2 is reversed by NADPH oxidase inhibition, Hypertension 56 (2010) 490–497.
[43] J.Y. Youn, L. Gao, H. Cai, The p47phox- and NADPH oxidase organiser 1 (NOXO1)-dependent activation of NADPH oxidase 1 (NOX1) mediates endothelial nitric oxide synthase (eNOS) uncoupling and endothelial dysfunction in a streptozotocin-induced murine model of diabetes, Diabetologia 55 (2012) 2069–2079.
[44] J.Y. Youn, J. Zhou, H. Cai, Bone morphogenic protein 4 mediates NOX1-dependent eNOS uncoupling, endothelial dysfunction, and COX2 induction in type 2 diabetes mellitus, Mol. Endocrinol. 29 (2015) 1123–1133.
[45] F. Rezende, F. Moll, M. Walter, V. Helfinger, F. Hahner, P. Janetzko, C. Ringel, A. Weigert, I. Fleming, N. Weissmann, C. Kuenne, M. Looso, M.A. Rieger, P. Nawroth, T. Fleming, R.P. Brandes, K. Schröder, The NADPH organizers NoxO1 and p47phox are both mediators of diabetes-induced vascular dysfunction in mice, Redox Biol 15 (2018) 12–21.
[46] S. Furukawa, T. Fujita, M. Shimabukuro, M. Iwaki, Y. Yamada, Y. Nakajima, et al., Increased oxidative stress in obesity and its impact on metabolic syndrome, J. Clin. Investig. 114 (2004) 1752–1761.
[47] J. Du, L.M. Fan, A. Mai, J.M. Li, Crucial roles of Nox2-derived oxidative stress in deteriorating the function of insulin receptors and endothelium in dietary obesity of middle-aged mice, Br. J. Pharmacol. 170 (2013) 1064–1077.
[48] C.M. Lynch, D.A. Kinzenbaw, X. Chen, S. Zhan, E. Mezzetti, J. Filosa, A. Ergul, J.L. Faulkner, F.M. Faraci, S.P. Didion, Nox2-derived superoxide contributes to cerebral vascular dysfunction in diet-induced obesity, Stroke 44 (2013) 3195–3201.
[49] P. Sukumar, H. Viswambharan, H. Imrie, R.M. Cubbon, N. Yuldasheva, M. Gage, S. Galloway, A. Skromna, P. Kandavelu, C.X. Santos, V.K. Gatenby, J. Smith, D.J. Beech, S.B. Wheatcroft, K.M. Channon, A.M. Shah, M.T. Kearney, Nox2 NADPH oxidase has a critical role in insulin resistance-related endothelial cell dysfunction, Diabetes 62 (2013) 2130–2134.
[50] A.M. Mahmoud, M.M. Ali, E.R. Miranda, J.T. Mey, B.K. Blackburn, J.M. Haus, S.A. Phillips, Nox2 contributes to hyperinsulinemia-induced redox imbalance and impaired vascular function, Redox Biol 13 (2017) 288–300.
[51] Y. Fu, R. Zhang, D. Lu, H. Liu, K. Chandrashekar, L.A. Juncos, R. Liu, NOX2 is the primary source of angiotensin II-induced superoxide in the macula densa, Am. J. Physiol. Regul. Integr. Comp. Physiol. 298 (2010) R707–R712.
[52] E. Babilonia, D. Lin, Y. Zhang, Y. Wei, P. Yue, W.H. Wang, Role of gp91phox -containing NADPH oxidase in mediating the effect of K restriction on ROMK channels and renal K excretion, J. Am. Soc. Nephrol. 7 (2007) 2037–2045.
[53] A.A. Eid, Y. Gorin, B.M. Fagg, R. Maalouf, J.L. Barnes, K. Block, H.E. Abboud, Mechanisms of podocyte injury in diabetes: role of cytochrome P450 and NADPH oxidases, Diabetes 58 (2009) 1201–1211.
[54] A.J. Valente, Q. Zhou, Z. Lu, W. He, M. Qiang, W. Ma, G. Li, L. Wang, B. Banfi, K. Steger, K.H. Krause, R.A. Clark, S. Li, Regulation of NOX1 expression by GATA, HNF-1alpha, and Cdx transcription factors, Free Radic. Biol. Med. 44 (2008) 430–433.
[55] S.P. Gray, J.C. Jha, K. Kennedy, E. van Bommel, P. Chew, C. Szyndralewiez, R.M. Touyz, H.H.H.W. Schmidt, M.E. Cooper, K.A.M. Jandeleit-Dahm, Combined NOX1/4 inhibition with GKT137831 in mice provides dose-dependent reno- and atheroprotection even in established micro- and macrovascular disease, Diabetologia 60 (2017) 927–937.
[56] T. Schlüter, U. Zimmermann, C. Protzel, B. Miehe, K.J. Klebingat, R. Rettig, O. Grisk, Intrarenal artery superoxide is mainly NADPH oxidase-derived and modulates endothelium-dependent dilation in elderly patients, Cardiovasc. Res. 85 (2010) 814–824.
[57] A.E. Dikalova, M.C. Góngora, D.G. Harrison, J.D. Lambeth, S. Dikalov, K.K. Griendling, Upregulation of Nox1 in vascular smooth muscle leads to impaired endothelium-dependent relaxation via eNOS uncoupling, Am. J. Physiol. Heart Circ. Physiol. 299 (2010) 673–679.
[58] J.Y. Youn, L. Gao, H. Cai, The p47phox- and NADPH oxidase organiser 1 (NOXO1)-dependent activation of NADPH oxidase 1 (NOX1) mediates endothelial nitric oxide synthase (eNOS) uncoupling and endothelial dysfunction in a streptozotocin-induced murine model of diabetes, Diabetologia 55 (2012) 2069–2079.